

Ruthenium Complexes Containing Chiral N-Donor Ligands as Catalysts in Acetophenone Hydrogen Transfer – New Amino Effect on Enantioselectivity

Montserrat Gómez,^{*[a]} Susanna Jansat,^[a] Guillermo Muller,^[a] Gabriel Aullón,^[a] and Miguel Angel Maestro^[b]

Keywords: Ruthenium / Chiral N-donors / Asymmetric catalysis / NMR spectroscopy / Density functional calculations

New *p*-cymene ruthenium species containing chiral amino alcohols (**1–3**), primary (**4–7**) and secondary (**8, 9**) amino-oxazolines, were tested as catalysts in the hydrogen transfer of acetophenone, using 2-propanol as the hydrogen source. A remarkable effect on the enantioselectivity, but also on the activity, was observed depending on the amino-type oxazoline, Ru/**8** and Ru/**9** being low active and nonselective catalytic systems, in contrast to their primary counterpart Ru/**5**. Complexes containing amino-oxazolines (**10–12**) were prepared and fully characterized, both in solution and in solid state. The X-ray structure was determined for (*S*_{Ru},*R*_C)-**10**.

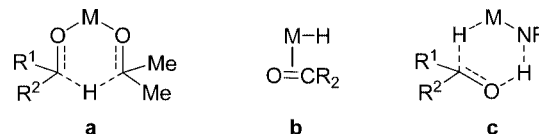
The diastereomeric ratios observed for complexes **10** and **11** were determined by ¹H NMR and confirmed by means of structural modeling (semi-empirical PM3(tm) level). DFT theoretical calculations for the transition states involved in the hydrogen transfer process proved the important differences in their relative populations, which could justify the enantioselectivity divergences observed between primary and secondary amino-oxazoline ruthenium systems.

(© Wiley-VCH Verlag GmbH & Co. KGaA, 69451 Weinheim, Germany, 2005)

Introduction

Chiral hydrogen transfer of prochiral ketones catalyzed by transition metals has emerged as a convenient methodology to give enantiomerically pure secondary alcohols, based on the simplicity of the process and the safety of the reagents.^[1]

From a mechanistic point of view, three alternatives have been proposed for metal-catalyzed hydrogen transfer of ketones (Scheme 1): i) direct transfer of a hydrogen atom of the alcohol to the carbonyl carbon through a concerted process involving a six-membered cyclic transition state (**a**), a mechanism accepted for Al-catalyzed Meerwein-Ponndorf-Verley reductions and generally for main group elements;^[2] ii) stepwise mechanism through the formation of a hydride metal intermediate and the migratory insertion of a C=O into a M–H bond (**b**), a mechanism suggested for rhodium(I) and ruthenium free-arene systems;^[3] and iii) a concerted mechanism where a proton and a hydride are simultaneously transferred to the unsaturated substrate (**c**), a mechanism proposed by Noyori for the Ru arene derivatives.^[4]



Scheme 1. Key species involved in the three main mechanisms [concerted (**a**) and (**c**), and stepwise (**b**)] of metal-catalyzed hydrogen transfer (spectator ligands on the metal have been omitted for clarity).

The efficient catalytic system described by Noyori and co-workers, Ru/TsDPEN (TsDPEN=*N*-(*p*-tolylsulfonyl)-1,2-diphenylethylenediamine), suggests the requirement of amino groups in order to achieve high activities.^[4,5] Other related works showed similar trends.^[6] In order to understand the reaction pathway, theoretical studies have been reported on the basis of the ruthenium complex structures and their reactivity, for systems containing primary and secondary amines.^[7] These systems are in agreement with a metal–ligand bifunctional mechanism.

We previously tested *p*-cymene ruthenium systems containing chiral bis(oxazolines) as catalysts in the acetophenone reduction processes, in particular in hydrogenation transfer.^[8] Moderated enantiomeric excesses were obtained (*ee* up to 38%), and the best chiral auxiliaries were found among those containing two carbon spacers between both oxazoline fragments. As stated above, the presence of NH₂ or NH groups in the auxiliaries is fundamental for catalytic reactivity.^[4b] For that reason, and following our research with oxazoline ligands,^[9] we proposed to use primary (**4–7**)

[a] Departament de Química Inorgànica, Universitat de Barcelona, Martí I Franquès 1-11, 08028 Barcelona, Spain
Fax: +34-93-4907725
E-mail: montserrat.gomez@qi.ub.es

[b] Departamento de Química Fundamental, Universidade da Coruña, Campus da Zapateira, s/n, 15071 A Coruña, Spain

and secondary (**8–9**) amino-oxazolines in order to improve the results previously obtained (Figure 1). The amino alcohol precursors of the corresponding oxazolines were also tested (**1–3**). In order to rationalize the catalytic results found, a structural study of ruthenium complexes was carried out, both in solution (by means of NMR spectroscopy) and in solid state (by means of X-ray diffraction). The diastereomeric distributions observed in solution were confirmed by structural modeling (PM3(tm) level). In addition, a theoretical study (DFT level) was also carried out con-

cerning the relative energies of the corresponding transition states responsible for the hydrogen transfer from catalytic species to the prochiral ketone.

Results and Discussion

Synthesis of Chiral Amino-Oxazoline Ligands

The optically pure amino-oxazolines **4** and **5** recently reported in the literature were prepared in one and three steps, respectively.^[10] The standard Zn-catalyzed condensation of anthranilonitrile with the appropriated amino alcohol, followed for the synthesis of **4**,^[10b] gave low yields for **5** and **6** (less than 30% after three days of reaction). But better results were obtained when the cyclization process took place under basic conditions in a mixture of glycerol and ethylenglycol in a one-step process (Scheme 2),^[11] in contrast to the three-step synthetic route from isatoic anhydride.^[10c] The one-pot synthesis gave a mixture of the expected oxazoline and the corresponding amide (oxazoline/amide 85:15 for **5** and 1:1 for **6**), which were separated by aqueous extractions (the oxazoline remains in the organic phase). The pure amide derived from L-valinol can be transformed to the corresponding oxazoline **5** by substitution of the hydroxyl group with *p*-tolylsulfonyl chloride and cyclization under basic conditions (0.5 M NaOH, in H₂O/MeOH 1:1) at room temperature for two days. The oxazoline **7** was easily obtained by silylation of **6** with SiClMe₃ in excellent yield. The secondary amine ligands, **8** and **9**, were obtained in two different synthetic ways. Ligand **8** was prepared from the primary amino-oxazoline **5** following the procedure described previously in the literature.^[12] But analogous methodology using methyl iodide in place of *p*-toluenesulfonyl chloride failed to give **9**, which was isolated in good yield

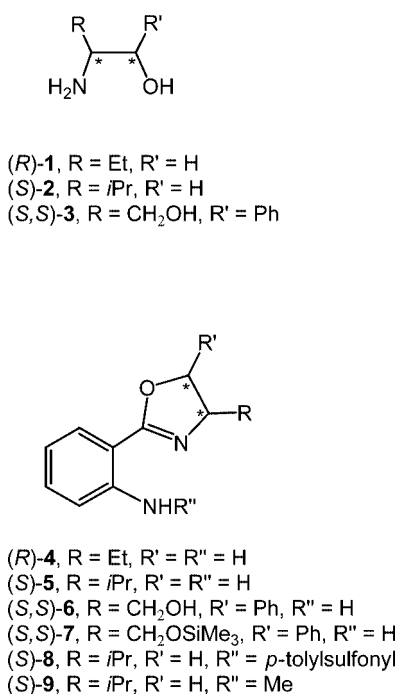
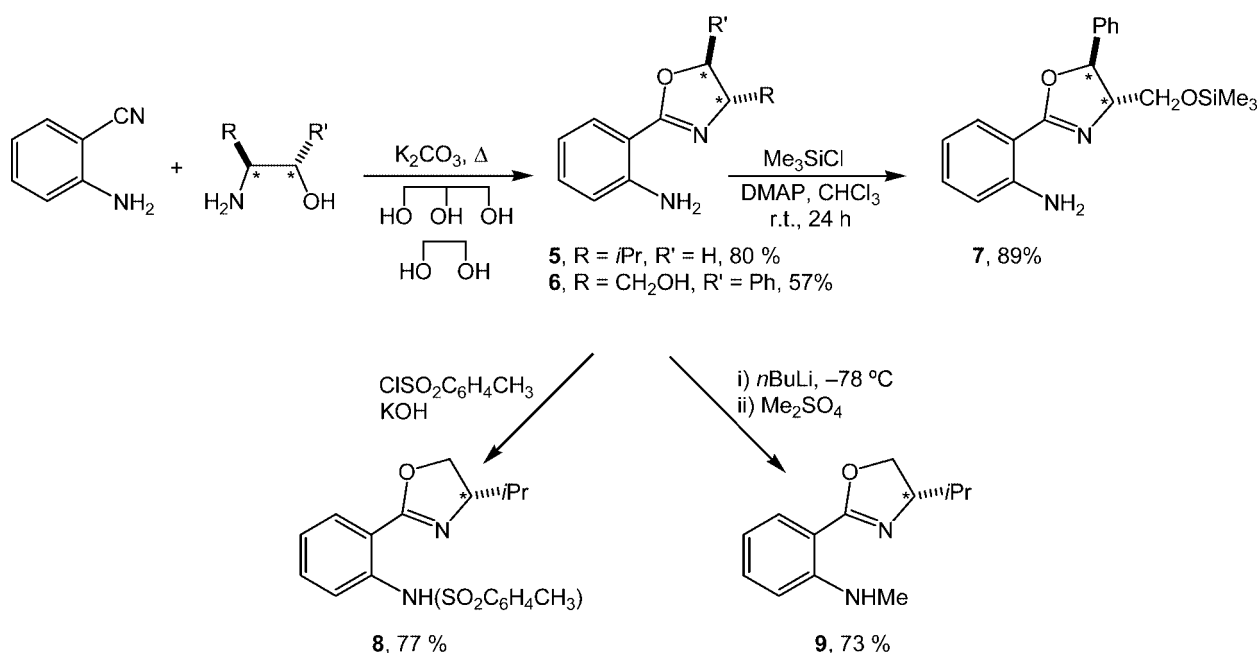


Figure 1. Chiral amino alcohols (**1–3**) and amino-oxazolines (**4–9**).

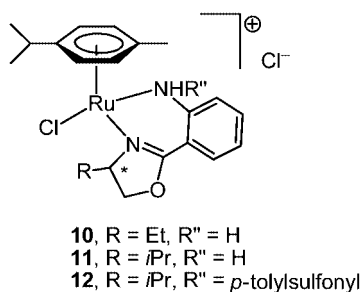
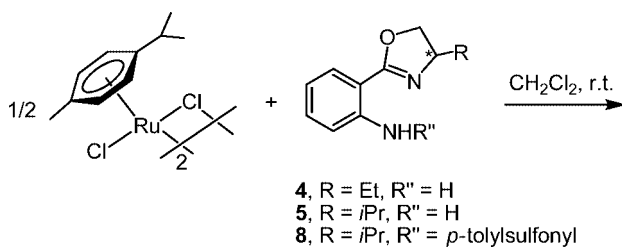


Scheme 2. Synthesis of primary (**5–7**) and secondary (**8–9**) chiral amino-oxazolines.

in two steps, reacting dimethyl sulfate with the lithium derivative of **5** (Scheme 2).

Ruthenium Complexes

The cationic complexes **10**, **11** and **12**, of general formula $[\text{RuCl}(p\text{-cymene})(\kappa^2\text{-}N,N\text{-}L)]\text{Cl}$ (where $L = \mathbf{4}, \mathbf{5}$ and $\mathbf{8}$, respectively) were synthesized from the dimeric p -cymene precursor and the appropriated amino-oxazoline (Scheme 3). Complexes **10** and **11** were obtained as a mixture of two diastereomers, since the ruthenium chiral center formed upon coordination of optically pure oxazoline ligand: $(S_{\text{Ru}}, R_{\text{C}})^-$ + $(R_{\text{Ru}}, R_{\text{C}})^-$ -**10** and $(S_{\text{Ru}}, S_{\text{C}})^-$ + $(R_{\text{Ru}}, S_{\text{C}})^-$ -**11**, as observed for analogous arene Ru complexes containing pyridino-oxazolines.^[13] In solution, complex **12** shows at least three isomers, probably due to the N stereocenter. The complexes were fully characterized both in solid state and solution.



Scheme 3. Synthesis of ruthenium complexes (**10–12**) containing amino-oxazolines (**4**, **5**, **8**).

Single crystals of **10** were obtained by slow diffusion of hexane over a chloroform/dichloromethane solution of the complex (Figure 2). Selected bond lengths and angles are listed in Table 1. The absolute configuration of the ruthenium stereocenter is S_{Ru} [according to the priority sequence $\eta^6\text{-arene} > \text{Cl} > \text{N}_{\text{ox}}(1) > \text{N}_{\text{amino}}(2)$].^[14] The complex adopts a distorted three-legged “piano stool” geometry. The ruthenium atom is η^6 -coordinated to the p -cymene unit (calculated distance between the planar arene group and metal is 1.66 Å), and the other three positions are occupied by the two nitrogen (from the bidentated ligand) and chlorine atoms. The bond distances and angles are quite similar to those for the known analogous ruthenium complexes.^[15] It is interesting to note the short intramolecular nonbonded distances of one amino hydrogen atom (H1B) with the oxazoline nitrogen and chlorine atoms: $\text{N}_{\text{amino}}(1)\text{--H}(1\text{B})\cdots$

$\text{Cl}(1) = 2.62 \text{ \AA}$ and $\text{N}_{\text{amino}}(1)\text{--H}(1\text{B})\cdots\text{N}_{\text{ox}}(2) = 2.79 \text{ \AA}$, shorter than the expected van der Waals separations (3.0 Å),^[16] and consistent with hydrogen bonds.^[17,18] These distances are significantly shorter than for H(1A): $\text{N}_{\text{amino}}(1)\text{--H}(1\text{A})\cdots\text{Cl}(1) = 2.85 \text{ \AA}$ and $\text{N}_{\text{amino}}(1)\text{--H}(1\text{A})\cdots\text{N}_{\text{ox}}(2) = 3.30 \text{ \AA}$ (the hydrogen positions were calculated, not found in the difference Fourier map). It is also significant that the nitrogen–axial hydrogen distance ($\text{N--H}(1\text{B}) = 0.862 \text{ \AA}$) is shorter than the nitrogen–equatorial hydrogen one ($\text{N--H}(1\text{A}) = 0.869 \text{ \AA}$), as observed for other related compounds.^[5b]

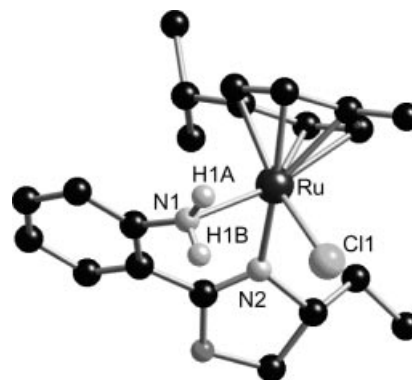


Figure 2. Molecular structure and atom labeling scheme for the cation of $(S_{\text{Ru}}, R_{\text{C}})$ -**10**. Hydrogen atoms, except H1A, H1B, and the chloride contra-anion have been omitted for clarity.

Table 1. Selected bond lengths [Å] and angles [°] for $(S_{\text{Ru}}, R_{\text{C}})$ -**10** (with esd's in parentheses).

Ru(1)–N(2)	2.110(7)
Ru(1)–N(1)	2.135(6)
Ru(1)–Cl(1)	2.401(2)
Ru(1)–C(17)	2.168(8)
Ru(1)–C(13)	2.177(8)
Ru(1)–C(16)	2.184(8)
Ru(1)–C(14)	2.209(8)
Ru(1)–C(15)	2.212(8)
Ru(1)–C(12)	2.225(9)
N(2)–Ru(1)–N(1)	80.5(3)
N(2)–Ru(1)–Cl(1)	83.2(2)
N(1)–Ru(1)–Cl(1)	83.7(2)

Conductivity measurements in acetonitrile for complexes **10** and **11** show the existence of 1:1 electrolytes in solution (about $50 \text{ \Omega}^{-1} \text{ cm}^2 \text{ mol}^{-1}$).^[19] The highest peak of positive FAB mass spectra corresponds to the cation $[\text{RuCl}(p\text{-cymene})\text{L}]^+$ ($L = \mathbf{4}$ for **10**; $L = \mathbf{5}$ for **11**).

¹H NMR spectra for both ruthenium complexes indicate the existence of two isomers in about 5:1 and 2:1 ratios for **10** and **11**, respectively. For complex **10** many signals appeared overlapped and consequently a complete assignment for both isomers was not possible, in contrast to complex **11** (see Experimental section for NMR spectroscopic data). The N_{amino} -coordination of the oxazoline ligand in **11** is proven by the different chemical shifts of the two N–H protons, for each isomer, analogously to Ru arene complexes containing amino alcohols.^[20] The difference between both chemical shifts (more than 5 ppm) stands out, due to the intramolecular hydrogen bond between one N–H and the

Table 2. Asymmetric hydrogen transfer of acetophenone catalyzed by chiral ruthenium systems, Ru/L* (L* = 1–9).^[a]

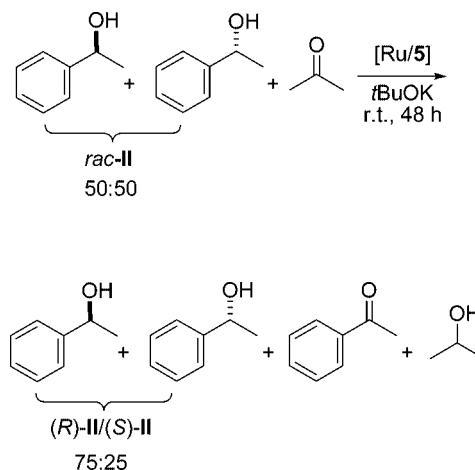
Entry	L*	I/Ru	Time (h)	Conv. (%) ^[b]	ee II (%) ^[b]	TOF (h ⁻¹) (%)
1	1	100/1	1.5	89	12 (<i>R</i>)	59
2	2	100/1	1.5	80	32 (<i>S</i>)	53
3	2	20/1	0.5	92	32 (<i>S</i>)	37
4	3	100/1	24	0	–	–
5	3	20/1	72	17	33 (<i>S</i>)	0.2
6 ^[c]	4	20/1	24	20	43 (<i>R</i>)	0.2
7	5	20/1	1.5	53	45 (<i>S</i>)	7.0
8	5	20/1	24	75	45 (<i>S</i>)	0.6
9	5	20/1	72	33	79 (<i>S</i>)	0.1
10	6	20/1	1.5	9	n.d.	
11 ^[c]	6	20/1	24	41	2.0	1.2
12 ^[c]	7	20/1	1.5	95	71 (<i>S</i>)	0.3
13	8	20/1	1.5	3	nd	0
14	8	20/1	24	63	0	0.5
15 ^[c]	8	20/1	72	92	0	0.3
16	9	20/1	1.5	12	0	1.6
17 ^[c]	9	20/1	24	42	0	0.3

[a] Results from duplicated experiments. Ru/L*/*t*BuOK 1:2:3. See Scheme 4. [b] Conversions based on the substrate **I** and enantiomeric excesses (absolute configuration in parenthesis) determined by GC. [c] Reaction monitored up to 120 h, being conversion and enantioselectivity constants.

1 and 2 vs 4 and 5), in contrast to the results observed with α,β -dialkyl-substituted amino alcohols.^[20] In our case the introduction of a second alcohol function leads to a dramatic activity decrease, but with an asymmetric induction similar to ligand **2** (entries 2 and 5). The selectivity of Ru/**1** and Ru/**2** systems is independent of the acetophenone/ruthenium ratio (entries 2 and 3). When the ruthenium-to-ligand ratio was 1:1, the catalytic behavior did not change, proving that the catalytic species are active without the ligand excess in the reaction medium that was observed previously for other ligands.^[23]

Amino-oxazolines **4** and **5** are less active but more selective than the corresponding amino alcohols **1** and **2** (entries 6 and 7 vs 1 and 2, respectively). Also, oxazoline **6** is more selective than **3** (entry 11 vs 5), and, in turn, the silyl oxazoline **7** is more active than **6** (entry 12 vs 10 and 11), the Ru/**7** system being the most active oxazoline catalyst tested. These results indicate a “poison” effect of the alcohol group, both for the amino alcohol **3** and the oxazoline derivative **6**. In addition, we observe that the catalytic activity and selectivity are highly influenced by the substitution degree of the oxazoline heterocycle (**7**, α,β -disubstituted oxazoline, is more active and affords better enantiomeric excesses than **4** and **5**, β -monosubstituted oxazolines), as reported for α,β -dialkyl-substituted amino alcohols.^[20]

We note that only the Ru/**5** catalytic system leads to an increase of enantiomeric excess (up to 79%) at long reaction times, together with a conversion decrease (entries 8 and 9). This proves the reversibility of the transfer hydrogenation, as stated by Noyori.^[4a,24] In order to verify this kinetic resolution, the dehydrogenative oxidation of *rac*-**II** with acetone was carried out under similar conditions as those described above for the direct process (Scheme 5). After 48 h at room temperature, 46% of acetophenone was formed, achieving an enantiomeric excess for 1-phenylethanol up to 50% (*S*); then (*R*)-**II** dehydrogenates faster than the (*S*)-**II** enantiomer.



Scheme 5. Dehydrogenative oxidation of *rac*-**II** catalyzed by the Ru/**5** system.

Secondary amino-oxazolines, *N*-(*p*-tolylsulfonyl)- and *N*-methyl-amino-oxazoline (**8** and **9**, respectively), were somewhat less active than the analogous primary amino-oxazoline **5** (entries 14 and 17 vs 8), and what is more significant, they did not induce asymmetry (entries 13–17). Then a primary amine moiety and not a secondary amine function in the ligand appears essential for the enantioselectivity. This is something that has not been observed before and is only mentioned for indanol amino alcohol derivatives.^[6c]

Theoretical Calculations

Assuming that the Ru-catalyzed hydrogen transfer process involves a concerted transfer of both proton and hydride, a six-membered transition state may be responsible for the ketone reduction by means of a double hydrogen transfer from Ru–H and N–H bonds towards the prochiral substrate, as postulated by Noyori.^[7a,25] This concerted

mechanism for Ru complexes containing bidentated N-donor ligands, in particular oxazolinyI (N_{ox})-amino(NHR) ligands, is represented in Figure 4.

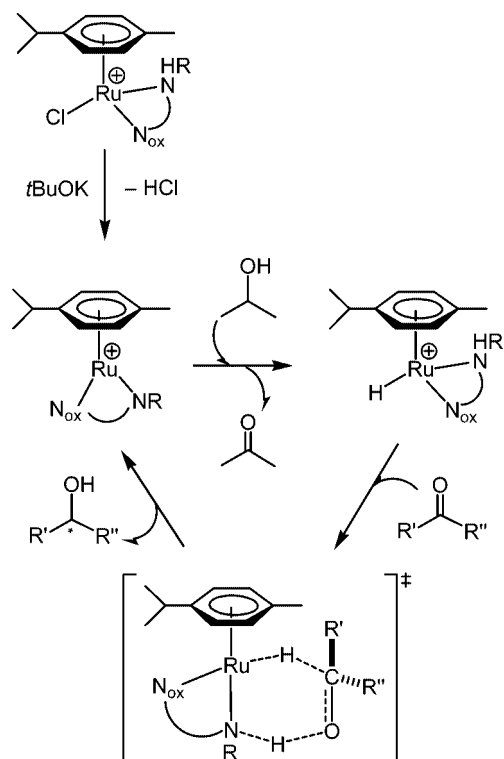


Figure 4. Catalytic cycle for Ru-catalyzed hydrogen transfer of ketones through a concerted mechanism.

For prochiral substrates, like the acetophenone, the enantiomeric enhancement of the chiral alcohol formed depends on the way that the ketone enantioface approaches the metal-hydride intermediate (see transition states depicted in Figure 5). In order to understand the enantioselectivity differences observed with our catalytic systems containing substituted (NHR for ligands **8** and **9**) and nonsubstituted (NH_2 for **4**–**7**) amino groups, theoretical calculations at DFT level were carried out for the corresponding transition states (see below). In the hydride model structure **13** (Figure 5), the substituent on the oxazoline stereocenter is a methyl group with *S* absolute configuration. The energy difference between both optimized diastereomers was $0.59 \text{ kcal mol}^{-1}$ (Boltzmann distribution, 73:27), the S_{Ru} being the most stable isomer, where the oxazoline substituent at the stereocenter points away from the arene group, analogously to the related prepared chloro complexes **10** and **11** (see above).

The calculated transition states are labeled as **TS- R_{II} -13** or **TS- S_{II} -13** depending on the 1-phenylethanol enantiomer afforded (Figure 5). Their relative stability of four transition states are determined by an equilibrium between weak hydrogen interactions of the type $C-H \cdots Ar$. Our calculations show that the two most stable states produce the *R* alcohol (relative energies are 0.0 and $+1.2 \text{ kcal mol}^{-1}$), whereas the relative *S* alcohol states are higher in energy ($+1.6$ and $+2.5 \text{ kcal mol}^{-1}$). Concerning the transition states related to the **13** hydride species, the Boltzmann distribution (298 K) for their four transition states leads to a calculated enantiomeric excess for the secondary alcohol **II** of about 40% in the *R* isomer (Figure 6), in agreement with the catalytic results obtained with the analogous amino-oxazolines con-

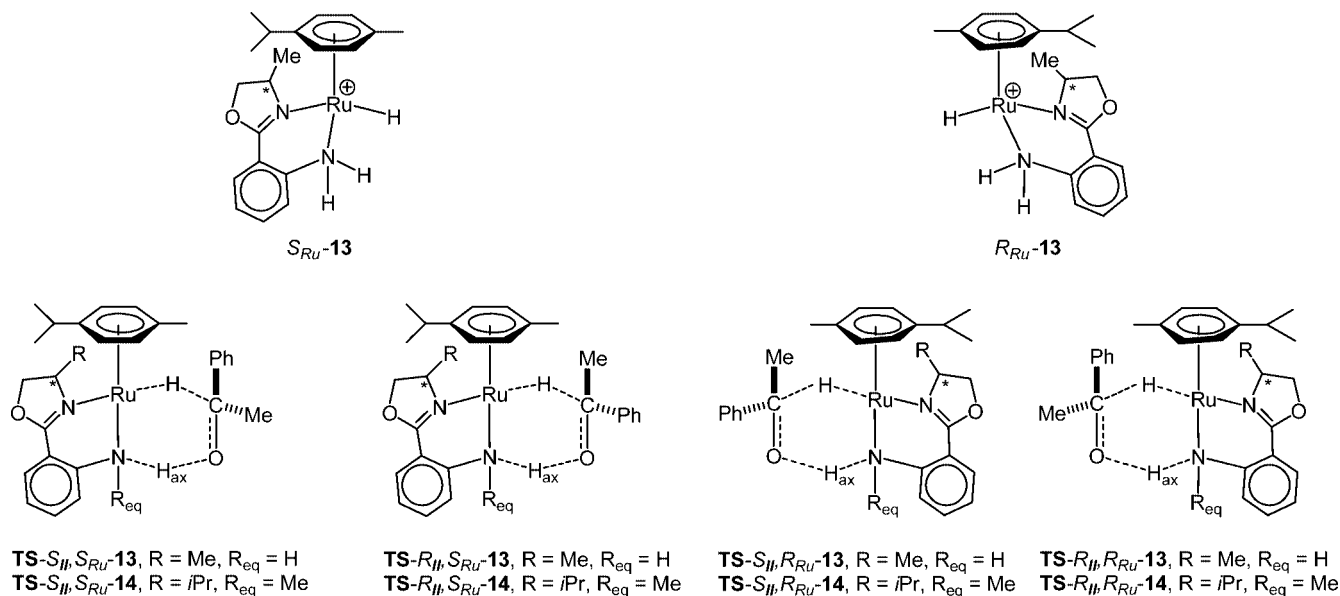


Figure 5. Optimized hydride species **13** (S_{Ru} -**13** and R_{Ru} -**13**) and the transition states involved in the hydrogenation of acetophenone used in the DFT study.

taining an ethyl and isopropyl instead of the methyl group (ligands **4** and **5**).

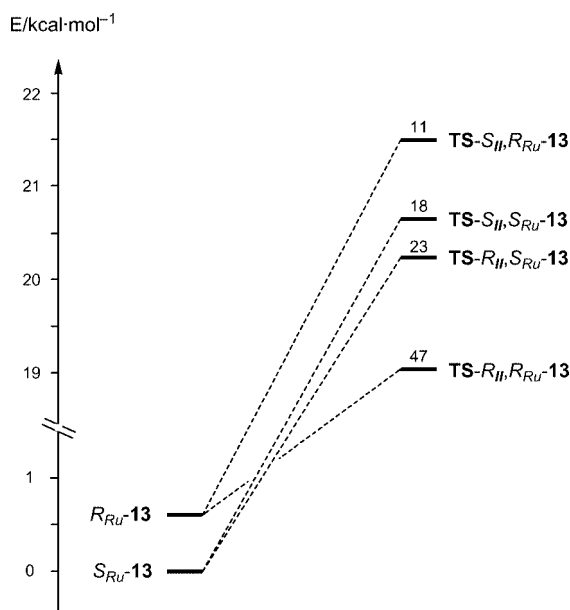


Figure 6. Energy profile for minima of compound model **13**, and their generated transition states (Figure 5) for the reaction with acetophenone, depending on the relative orientation of prochiral ketone. Relative populations of transition states are shown according to the Boltzmann distribution at 298 K.

The good correlation observed between experimental and calculated data for the Ru systems containing primary amino ligands led us to calculate the relative population of the transition states involved with Ru species containing secondary amino-oxazoline **9** (transition states labeled as **14**

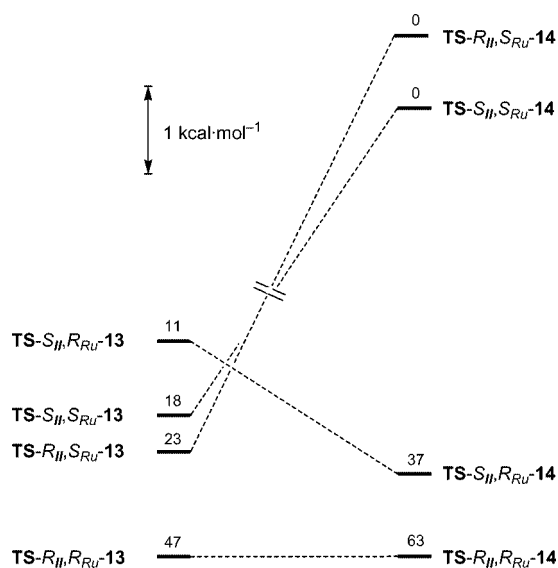


Figure 7. Relative stabilities of Ru transition states involved in the acetophenone hydrogen transfer containing primary (**13**) and secondary (**14**) oxazolinyl-amines. Relative populations are shown as Figure 5 and zero level is taken from the $TS-R_{II},R_{Ru}$ isomer.

in Figure 5). For these states, only the two axial related species were taken into account because of the topological arrangement for hydrogen transfer to the prochiral ketone in the transition state (Figure 5). As depicted in Figure 7, the isomers $TS-S_{Ru}$ -**14** are less stable than the other two, possibly due to steric repulsions, having an energy higher than 10 kcal mol⁻¹ and higher than the related $TS-R_{Ru}$ -**14**. For this reason they do not play any role in our catalytic system (Figure 8). Consequently, only the lowest transition states, $TS-R_{II},R_{Ru}$ -**14** and $TS-S_{II},R_{Ru}$ -**14**, participate in the hydrogenation reaction and the small energy gap between the two forms is responsible for a decrease of enantiomeric excess (calculated *ee* = 26%). In contrast, in the related transition states of **13**, the largest populations corresponded to the transition states leading to the *R* enantiomers, explaining the selectivity trends observed for Ru catalytic systems containing primary and secondary amino-oxazolines (see Catalytic section).

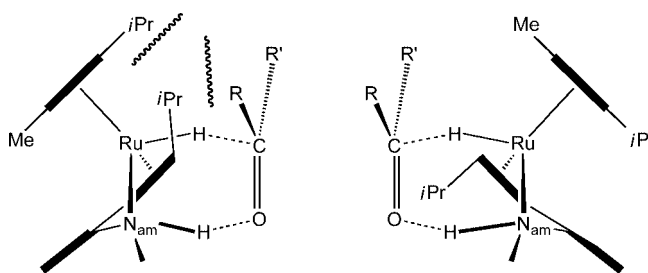


Figure 8. Schematic representation of the transition states $TS-14$. The steric repulsions between hydrocarbon groups for $TS-S_{Ru}$ -**14** (left) are missing in analogous $TS-R_{Ru}$ -**14** (right).

Conclusions

We used modular chiral N-donor ligands in order to study the fine effects on the transfer hydrogenation of acetophenone catalyzed by Ru arene systems. An important influence on selectivity was found to depend on the nature of the amino group: secondary amino ligands (**8–9**) do not induce enantioselectivity, in contrast to their analogous primary derivative (**5**). In order to rationalize these results, a structural and mechanistic study was proposed. The synthesis and full characterization of complexes containing primary (**10** and **11**) and secondary (**12**) oxazolinyl-amino ligands was carried out. The NMR spectroscopic data show the presence of isomers due to the new stereocenters (Ru and also N for **12**) generated upon coordination of the ligands (**4**, **5**, and **8**) to the metal. The relative populations found by modeling structures (PM3(tm) level) are in agreement with the diastereomeric ratios observed by NMR spectroscopy. The enantioselectivity loss observed for secondary amines relative to the analogous primary ligands can be justified by the theoretical data obtained (DFT studies) for the transition states proposed for the arene ruthenium systems involved in the hydrogen transfer of prochiral ketones.

Experimental Section

General Remarks: All compounds were prepared under purified nitrogen using standard Schlenk and vacuum-line techniques. The solvents were purified by standard procedures and distilled under nitrogen.^[26] (*R*)-(+)-2-Aminobutanol (Fluka), L-valinol (Aldrich), and [RuCl(*p*-cymene)(μ -Cl)]₂ (Aldrich) were used without previous purification. Ligand **4**^[10b] was prepared as described previously. NMR spectra were recorded with Varian XL-500 (¹H, standard SiMe₄), Varian Gemini (¹H, 200 MHz; ¹³C, 50 MHz; standard SiMe₄), Bruker DRX 250 (¹³C, 62.9 MHz, standard SiMe₄), and Mercury 400 (¹H, 400 MHz; ¹³C, 100 MHz, standard SiMe₄) spectrometers, using CDCl₃ as solvent, unless stated otherwise. Chemical shifts were reported downfield from standards. IR spectra were recorded with a Nicolet 520 FTIR spectrometer. FAB mass chromatograms were obtained on a Fisons V6-Quattro instrument. The GC analyses were performed on a Hewlett-Packard 5890 Series II gas chromatograph (50 m Ultra 2 capillary column) with a FID detector. Enantiomeric excesses were determined by GC on a FS-cyclodex- β -I/P column. Optical rotations were measured on a Perkin-Elmer 241MC spectropolarimeter. Conductivities were obtained on a Radiometer CDM3 conductimeter. Elemental analyses were carried out by the *Serveis Científico-Tècnics de la Universitat de Barcelona* in an Eager 1108 microanalyzer.

(+)-(4'*S*)-2-(4'-Isopropyl-3',4'-dihydrooxazol-2'-yl)aniline (5): L-Valinol (0.743 g, 7.20 mmol), 2-aminobenzonitrile (0.500 g, 4.23 mmol), and potassium carbonate (0.054 g, 0.39 mmol) were successively introduced in a Schlenk, followed by a solution of glycerol (5 mL) in dry ethylene glycol (9 mL). The resulting mixture was brought to 105 °C under nitrogen. The disappearance of the nitrile was followed by thin-layer chromatography (hexane/ethyl acetate, 3:1). After 24 h, the reaction was complete. Two new spots appeared on the thin layer, which were further identified as the amide for the high *R_f* and the oxazoline for the low *R_f* one (15:85 respectively, determined by GC analysis). The mixture was cooled to room temperature and then poured over crushed ice. The resulting white solid was filtered, dissolved in dichloromethane and, after several extractions with water, the organic phases were dried with anhydrous Na₂SO₄. Solvent elimination under low pressure gave the product as a white solid. Yield: 0.860 g (80%). IR (KBr): $\tilde{\nu}$ = 3395 (N–H), 3261 (N–H), 1640 (C=N), 1255 (C–O) cm⁻¹. ¹H NMR (250 MHz, CDCl₃; multiplicity, coupling constants in Hz, and relative integration in parentheses): 7.67 (pdd, 8.8, 1.6, 1 H), 7.19 (pt, 7.4, 1 H), 6.69 (m, 2 H), 6.13 (br. s, 2 H), 4.32 (ppd, 8.6, 7, 1 H), 4.11 (m, 1 H), 4.00 (t, 7.3, 1 H), 1.81 (m, 1 H), 1.03 (d, 6.8, 3 H), 0.93 (d, 6.8, 3 H) ppm. ¹³C NMR (50 MHz, CDCl₃): 163.4 (C), 148.5 (C), 131.8 (C), 129.5 (CH), 115.9 (CH), 115.5 (CH), 109.1 (CH), 72.9 (CH), 68.7 (CH₂), 33.2 (CH), 19.1 (CH₃), 18.6 (CH₃) ppm. C₁₂H₁₆N₂O (204): calcd. C 70.58, H 7.84, N 13.72; found C 70.29, H 8.02, N 13.74. MS (FAB positive) *m/z* 204 ([M]⁺). Melting point: 103 °C. [α]_D²⁵ (1 \times 10⁻³ M, CHCl₃) = +19.8.

(+)-(3'*S*,4'*S*)-2-(3'-Phenyl-4'-hydroxymethyl-3',4'-dihydrooxazol-2'-yl)aniline (6): (1*S*,2*S*)-2-Amino-1-phenyl-1,3-propanediol (1.201 g, 7.20 mmol), 2-aminobenzonitrile (0.500 g, 4.23 mmol), and potassium carbonate (0.054 g, 0.39 mmol) were successively introduced in a Schlenk, followed by a solution of glycerol (5 mL) in dry ethylene glycol (9 mL). The resulting mixture was brought to 105 °C under nitrogen. The disappearance of the nitrile was followed by thin-layer chromatography (hexane/ethyl acetate, 3:1). The reaction was complete after 36 h. Two new spots appeared on the thin layer, which were further identified as the amide for the high *R_f* and the oxazoline for the low *R_f* one (1:1 respectively, determined by GC analysis). The mixture was cooled to room tempera-

ture and washed with a saturated aqueous solution of NH₄Cl and extracted with dichloromethane (3 \times 15 mL). The organic extracts were dried with anhydrous Na₂SO₄. Solvent elimination under low pressure gave the product as a yellow oil. Yield: 0.640 g (57%). IR (NaCl): $\tilde{\nu}$ = 3466 (N–H), 3415 (O–H), 3309 (N–H), 1633 (C=N), 1261 (C–O) cm⁻¹. ¹H NMR (200 MHz, CDCl₃; multiplicity, coupling constants in Hz, and relative integration in parentheses): 7.81 (dd, 7.9, 0.6, 1 H), 7.24 (m, 3 H), 6.70 (m, 5 H), 6.07 (br. s, 2 H), 4.39 (d, 7, 1 H), 4.26 (pq, 3.6, 1 H), 3.94 (pdd, 11.5, 3.7, 1 H), 3.74 (dd, 11.2, 4.0, 1 H), 2.61 (br. s, 1 H) ppm. ¹³C NMR (50 MHz, CDCl₃): 164.8 (C), 148.6 (C), 140.8 (C), 132.4 (CH), 129.9 (CH), 128.8 (CH), 128.2 (CH), 125.6 (CH), 116.4 (CH), 115.9 (CH), 108.8 (C), 80.9 (CH), 64.1 (CH₂) ppm. MS (FAB positive) *m/z* 267 ([M–H]⁺). [α]_D²⁵ (1 \times 10⁻³ M, CHCl₃) = +59.3.

(+)-(3'*S*,4'*S*)-2-(3'-Phenyl-4'-trimethylsilyloxymethyl-3',4'-dihydrooxazol-2'-yl)aniline (7): Compound **6** (0.330 g, 1.23 mmol), imidazole (0.175 g, 2.58 mmol), DMAP (6.6 mg, 5.3 \times 10⁻² mmol), and SiClMe₃ (0.132 g, 1.22 mmol) were successively introduced in a Schlenk. The solids were dissolved in 50 mL of freshly distilled chloroform, and the resulting mixture was stirred for 24 h at room temperature. The evolution of the reaction was followed by thin-layer chromatography (hexane/ethyl acetate, 2:1). When the reaction was over, the organic phase was treated successively with 10 mL of saturated aqueous solution of sodium hydrogenocarbonate and 10 mL of a saturated aqueous solution of brine, and the organic extracts were then dried with anhydrous Na₂SO₄. After solvent evaporation, the resulting oil was purified by column chromatography on silica using a mixture of hexane/ethyl acetate (2:1) as eluent. The product was obtained as a white solid. Yield: 0.372 g (89%). IR (KBr): $\tilde{\nu}$ = 3408 (N–H), 3276 (N–H), 1635 (C=N), 1261 (C–O) cm⁻¹. ¹H NMR (200 MHz, CDCl₃; multiplicity, coupling constants in Hz, and relative integration in parentheses): 7.67 (pdd, 7.9, 1.5, 2 H), 7.16 (m, 4 H), 6.58 (d, 8.6, 2 H), 6.54 (pt, 7.6, 1 H), 5.97 (br. s, 2 H), 5.29 (d, 6.0, 1 H), 4.15 (m, 1 H), 3.83 (dd, 10.4, 4.2, 1 H), 3.55 (pdd, 10.1, 7.3, 1 H), –0.02 (s, 9 H) ppm. ¹³C NMR (50 MHz, CDCl₃): 164.2 (C), 148.8 (C), 141.5 (C), 132.2 (CH), 129.8 (CH), 128.6 (CH), 127.9 (CH), 125.0 (CH), 116.0 (CH), 115.6 (CH), 108.9 (C), 81.6 (CH), 77.2 (CH), 64.9 (CH₂), 0.1 (CH₃) ppm. C₁₉H₂₅N₂O₂Si (341.5): calcd. C 67.03, H 7.05, N 8.23; found C 67.69, H 7.11, N 8.30. MS (FAB positive) *m/z* 340 ([M]⁺). Melting point: 153 °C. [α]_D²⁵ (1 \times 10⁻³ M, CHCl₃) = +30.7.

(+)-(4'*S*)-2-(4'-Isopropyl-3',4'-dihydrooxazol-2'-yl)-*N*-(*p*-tolylsulfonyl)aniline (8): Stirring a solution of **5** (0.100 g, 0.49 mmol) and *p*-tolylsulfonyl chloride (0.160 g, 0.84 mmol) in dichloromethane with an aqueous solution of KOH (0.049 g, 0.89 mmol) for 8 h gave a white solid, which was filtered off and purified by column chromatography on silica using hexane/ethyl acetate (5:1) as eluent. Yield: 0.134 g (77%). IR (KBr): $\tilde{\nu}$ = 3389 (N–H), 1637 (C=N), 1341 (S=O), 1163 (S=O) cm⁻¹. ¹H NMR (200 MHz, CDCl₃; multiplicity, coupling constants in Hz, and relative integration in parentheses): 12.54 (br. s, 1 H), 7.66 (d, 8.2, 2 H), 7.62 (m, 2 H), 7.26 (ptd, 7.8, 1.4, 2 H), 6.91 (ptd, 7.9, 1.0, 1 H), 4.28 (dd, 8.6, 7.4, 1 H), 4.06 (m, 1 H), 3.98 (m, 1 H), 2.26 (s, 3 H), 1.73 (m, 1 H), 0.98 (d, 6.6, 3 H), 0.88 (d, 6.6, 3 H) ppm. ¹³C NMR (50 MHz, CDCl₃): 164.8 (C), 142.5 (C), 137.8 (C), 135.4 (C), 132.3 (CH), 129.4 (CH), 129.1 (CH), 127.1 (CH), 122.1 (CH), 117.6 (CH), 72.3 (CH), 69.5 (CH₂), 33.1 (CH), 18.8 (CH₃), 18.6 (CH₃) ppm. C₁₉H₂₅N₂O₂S (342): calcd. C 63.68, H 6.14, N 7.81; found C 63.78, H 6.53, N 7.60. MS (FAB positive) *m/z* 340 ([M]⁺). Melting point: 129 °C. [α]_D²⁵ (1 \times 10⁻³ M, CHCl₃) = +82.1.

(4'*S*)-2-(4'-Isopropyl-3',4'-dihydrooxazol-2'-yl)-*N*-(methyl)aniline (9): Compound **5** (0.150 g, 0.73 mmol) was dissolved in 10 mL of

THF. The resulting mixture was cooled to $-78\text{ }^{\circ}\text{C}$ under nitrogen. After 30 min, *n*BuLi (0.55 mL, 0.88 mmol) was introduced in the Schlenk, followed by a solution of Me_2SO_4 (0.111 g, 0.88 mmol) in THF (3 mL). The resulting mixture was warmed to room temperature. The reaction was complete after 18 h. Two new spots appeared on the thin layer, which were further identified as the product for the high R_f and the oxazoline **5** for the low R_f one (70:30 respectively, determined by GC analysis). The mixture was dissolved in dichloromethane and after several extractions with an aqueous saturated solution of NH_4Cl and water, the organic phases were dried with anhydrous Na_2SO_4 . The resulting oil was purified by column chromatography on silica using hexane/ethyl acetate (20:1) as eluent. Solvent elimination under low pressure gave the product as a yellow oil. Yield: 0.116 g (73%). IR (KBr) = 3265 (N–H), 3171 (N–H), 2959 (C–H), 1636 (C=N), 1253 (C–O) cm^{-1} . ^1H NMR (200 MHz, CDCl_3 ; multiplicity, coupling constants in Hz, and relative integration in parentheses): 8.31 (br. s, 1 H), 7.63 (dd, 7.9, 1.8, 1 H), 7.23 (m, 1 H), 6.53 (m, 2 H), 4.21 (dd, 8.4, 7.0, 1 H), 4.03 (m, 1 H), 3.90 (q, 7.0, 1 H), 2.85 (d, 4.8, 3 H), 1.69 (m, 1 H), 0.94 (d, 6.6, 3 H), 0.84 (d, 6.6, 3 H) ppm. ^{13}C NMR (50 MHz, CDCl_3): 163.6 (C), 149.8 (C), 132.2 (CH), 129.6 (CH), 113.9 (CH), 109.6 (CH), 108.3 (C), 72.8 (CH), 68.3 (CH_2), 33.1 (CH), 29.4 (CH_3), 19.0 (CH_3), 18.5 (CH_3) ppm. MS (FAB positive) m/z 218 ($[\text{M}]^+$).

Chloro-(η^6 -*p*-cymene)-[(4'*S*)-2-(4'-ethyl-3',4'-dihydrooxazol-2'-yl)-aniline-*N,N*]ruthenium(II) Chloride (10): $[\text{RuCl}(p\text{-cymene})(\mu\text{-Cl})_2]$ (102 mg, 0.166 mmol) and **4** (63.5 mg, 0.33 mmol) were dissolved in dichloromethane (18 mL) and stirred at room temperature for 8 h. The solvent was then removed and the residue washed with diethyl ether. The product was recrystallized from dichloromethane and diethyl ether, giving an orange solid. Yield: 0.156 g (95%). IR (KBr) = 3414 (N–H), 3052 (N–H), 1630 (C=N), 1293 (C–O) cm^{-1} . ^1H NMR (250 MHz, CDCl_3 , 233 K; multiplicity, coupling constants in Hz, and relative integration in parentheses) $\delta = \text{major isomer}$: 9.84 (d, 10.0, 1.6, 2 H), 8.61 (d, 7.5, 1 H), 7.60 (m, 2 H), 7.31 (m, 1 H), 5.78 (br. s, 2 H), 5.69 (br. s, 2 H), 5.58 (br. s, 2 H), 4.86 (pt, 11.2, 1 H), 4.68 (br. s, 1 H), 4.29 (m, 1 H), 2.28 (br. s, 1 H), 2.07 (br. s, 1 H), 1.64 (s, 3 H), 0.95 (m, 9 H) ppm. $\delta = \text{minor isomer}$: 8.52 (d, 12.5, 1 H), 7.74 (d, 7.5, 1 H), 5.05 (m, 1 H), 2.54 (m, 1 H) ppm. ^{13}C NMR (63 MHz, CDCl_3) $\delta = \text{major isomer}$: 163.9 (C), 135.1 (CH), 129.7 (CH), 126.8 (CH), 123.6 (CH), 119.4 (CH), 107.1 (CH), 97.9 (CH), 83.8 (CH), 81.3 (CH), 73.9 (CH), 67.9 (CH_2), 31.0 (CH), 26.9 (CH_2), 18.2 (CH_3), 9.9 (CH_3) ppm. $\text{C}_{21}\text{H}_{28}\text{Cl}_2\text{N}_2\text{ORu}$ (496.4): calcd. C 50.70, H 5.63, N 5.63, Cl 14.26; found C 50.94, H 5.49, N 5.78, Cl 14.20. MS (FAB positive): m/z calcd. for $\text{C}_{21}\text{H}_{28}\text{Cl}_2\text{N}_2\text{ORu}$ $[\text{M}]^+$: 460.2; found 460.3. Melting point: $232\text{ }^{\circ}\text{C}$. Molar conductivity ($c = 0.001\text{ M}$, acetonitrile): $47\text{ }\Omega^{-1}\text{ cm}^2\text{ mol}^{-1}$.

Chloro-(η^6 -*p*-cymene)-[(4'*S*)-2-(4'-isopropyl-3',4'-dihydrooxazol-2'-yl)aniline-*N,N*]ruthenium(II) Chloride (11): $[\text{RuCl}(p\text{-cymene})(\mu\text{-Cl})_2]$ (102 mg, 0.166 mmol) and **5** (67.9 mg, 0.33 mmol) were dissolved in dichloromethane (18 mL) and stirred at room temperature for 8 h. The solvent was then removed and the residue washed with diethyl ether. The product was recrystallized from dichloromethane and diethyl ether, giving an orange solid. Yield: 0.161 g (95%). IR (KBr) = 3427 (N–H), 3045 (N–H), 1631 (C=N), 1394 (C–O) cm^{-1} . ^1H NMR (500 MHz, CDCl_3 , 298 K; multiplicity, coupling constants in Hz, and relative integration in parentheses) $\delta = \text{major isomer}$: 10.31 (d, 10.0, 1 H), 8.77 (d, 8.0, 1 H), 7.58 (m, 1 H), 7.54 (dd, 7.2, 1.5, 1 H), 7.27 (t, 7.5, 1 H), 5.98 (m, 2 H), 5.76 (d, 5.5, 1 H), 5.62 (d, 6.0, 2 H), 4.58 (dd, 8.0, 6.0, 1 H), 4.52 (m, 2 H), 4.45 (dd, 10.0, 8.0, 1 H), 4.34 (d, 10.0, 1 H), 2.51 (m, 1 H), 2.42 (m, 1 H), 1.92 (s, 3 H), 1.04 (pt, 7.2, 6 H), 0.98 (pt, 7.0, 6 H) ppm. $\delta = \text{minor isomer}$: 9.91 (d, 11.0, 1 H), 8.57 (d, 8.0, 1 H), 7.79 (dd, 7.2,

1.5, 1 H), 7.58 (m, 1 H), 7.30 (t, 7.5, 1 H), 5.89 (br. s, 2 H), 5.79 (d, 6.0, 1 H), 5.65 (d, 6.0, 1 H), 5.01 (d, 11.0, 1 H), 4.86 (pt, 9.5, 1 H), 4.70 (m, 1 H), 4.52 (m, 2 H), 2.84 (m, 1 H), 2.60 (m, 1 H), 1.84 (s, 3 H), 0.93 (d, 7.5, 3 H), 0.59 (d, 6.5, 3 H) ppm. ^{13}C NMR (CDCl_3 , 100 MHz) $\delta = \text{major isomer}$: 164.2 (C), 142.1 (C), 134.7 (C), 128.7 (CH), 126.7 (CH), 124.7 (CH), 119.4 (CH), 107.2 (CH), 84.4 (CH), 84.1 (CH), 81.1 (CH), 80.6 (CH), 71.4 (CH_2), 69.4 (CH_2), 31.2 (CH), 28.3 (CH), 22.1 (CH), 21.2 (CH), 19.7 (CH_3), 18.2 (CH), 15.0 (CH_3) ppm. $\delta = \text{minor isomer}$: 163.3 (C), 142.7 (C), 134.7 (C), 130.8 (CH), 126.8 (CH), 123.7 (CH), 118.7 (CH), 97.2 (CH), 84.0 (CH), 79.0 (CH), 78.3 (CH), 77.5 (CH), 69.5 (CH_2), 66.0 (CH_2), 30.9 (CH), 28.8 (CH), 23.3 (CH), 19.8 (CH_3), 18.1 (CH_3), 14.9 (CH_3) ppm. $\text{C}_{22}\text{H}_{30}\text{Cl}_2\text{N}_2\text{ORu}$ (475): calcd. C 51.76, H 5.88, N 5.49, Cl 13.90; found C 51.29, H 6.00, N 5.25, Cl 13.40. MS (FAB positive): m/z calcd. for $\text{C}_{22}\text{H}_{30}\text{Cl}_2\text{N}_2\text{ORu}$ $[\text{M}]^+$: 439.6; found 439.0. Melting point: $243\text{ }^{\circ}\text{C}$. Molar conductivity ($c = 0.001\text{ M}$, acetonitrile): $50\text{ }\Omega^{-1}\text{ cm}^2\text{ mol}^{-1}$.

Chloro-(η^6 -*p*-cymene)-[(4'*S*)-2-(4'-isopropyl-3',4'-dihydrooxazol-2'-yl)-*N*-(*p*-tolylsulfonyl)aniline-*N,N*]ruthenium(II) Chloride (12): $[\text{RuCl}(p\text{-cymene})(\mu\text{-Cl})_2]$ (9.6 mg, 0.015 mmol) and **8** (11.3 mg, 0.031 mmol) were dissolved in dichloromethane (4 mL) and stirred at room temperature for 8 h. The solvent was then removed and the residue washed with diethyl ether. The product was recrystallized from dichloromethane and diethyl ether, giving an orange solid. Yield: 0.019 g (99%). IR (KBr) = 3245 (N–H), 1634 (C=N), 1267 (SO_2), 1099 (SO_2) cm^{-1} . ^1H NMR (500 MHz, CDCl_3 , 298 K; multiplicity, coupling constants in Hz, and relative integration in parentheses) $\delta = \text{major isomer}$: 9.49 (br. s, 1 H), 8.30 (d, 8.0, 1 H), 7.60 (d, 7.0, 1 H), 7.58 (t, 7.8, 1 H), 7.37 (d, 6.5, 2 H), 7.32 (m, 1 H), 7.23 (q, 6.7, 2 H), 6.84 (m, 3 H), 6.26 (m, 3 H), 6.25 (d, 6.0, 1 H), 6.10 (d, 5.5, 1 H), 5.37 (d, 4.5, 1 H), 5.22 (d, 4.5, 1 H), 4.30 (t, 12.2, 1 H), 4.23 (d, 11.5, 1 H), 4.13 (d, 10.0, 1 H), 3.94 (d, 12.0, 1 H), 2.31 (m, 1 H), 1.23 (s, 3 H), 1.24 (m, 1 H), 0.98 (d, 6.5, 6 H), 0.85 (d, 6.0, 6 H), 0.29 (s, 3 H) ppm. $\text{C}_{29}\text{H}_{36}\text{Cl}_2\text{N}_2\text{O}_3\text{RuS}$ (664.6): calcd. C 52.41, H 5.45, N 4.21, S 4.82; found C 52.80, H 5.60, N 4.00, S 4.95. MS (FAB positive): m/z calcd. for $\text{C}_{29}\text{H}_{36}\text{Cl}_2\text{N}_2\text{O}_3\text{RuS}$ $[\text{M}]^+$: 629.20; found 629.00.

Ruthenium-Catalyzed Hydrogen Transfer of Acetophenone: The precursor ($[\text{Ru}(p\text{-cymene})\text{Cl}(\mu\text{-Cl})_2]$, 1.8 mg, 3×10^{-3} mmol) and ligand (12×10^{-3} mmol) were dissolved in a solution (2 mL, 0.012 M) of *t*BuOK in 2-propanol at room temperature for 30 min. Then a solution of acetophenone in 2-propanol (2 mL, 0.06 M) was added. The reaction was performed at room temperature under nitrogen, monitored by GC. When the Ru/substrate ratio was 1:100, the precursor (1.8 mg, 3×10^{-3} mmol) and ligand (12×10^{-3} mmol) were dissolved in a solution of *t*BuOK in 2-propanol (10 mL, 0.012 M) at room temperature for 30 min. Then a solution of acetophenone in 2-propanol (10 mL, 0.06 M) was added. The reaction was performed at room temperature under nitrogen, monitored by GC.

Ruthenium-Catalyzed Dehydrogenation of *rac*-1-Phenylethanol: The precursor (1.8 mg of $[\text{Ru}(p\text{-cymene})\text{Cl}(\mu\text{-Cl})_2]$, 3×10^{-3} mmol) and ligand **5** (25 mg, 12×10^{-3} mmol) were dissolved in a solution of *t*BuOK in 2-propanol (2 mL, 0.012 M) at room temperature for 30 min. Then an equimolar solution of *rac*-1-phenylethanol and acetone in 2-propanol (2 mL, 0.06 M) was added. The reaction was performed at room temperature under nitrogen, monitored by GC.

X-ray Crystallographic Study: An orange block of **10** was selected and mounted on a Bruker SMART CCD area detector single-crystal diffractometer with graphite monochromatized $\text{Mo-K}\alpha$ radiation ($\lambda = 0.71073\text{ \AA}$) operating at room temperature. Crystal data are summarized in Table 3.

Table 3. Crystal data for (S_{Ru}, R_C)-10.

	(S_{Ru}, R_C)-10
Empirical formula	C ₂₃ H ₂₉ Cl ₈ N ₂ ORu
Molecular mass	734.15
Crystal size [mm]	0.39 × 0.09 × 0.08
Temperature [K]	298(2)
Crystal system	orthorhombic
Space group	$P2_12_12_1$
a (Å)	8.881(1)
b (Å)	18.102(2)
c (Å)	20.231(2)
V [Å ³]	3252.6(5)
Z	4
Density (calculated) [Mg m ⁻³]	1.499
Absorption coefficient [mm ⁻¹]	1.158
θ range for data collection [°]	1.51–26.37
Reflections collected ($I \geq 2\sigma(I)$)	19013
Independent reflections	6599
Final R indices [$I > 2\sigma(I)$] ^[a]	$R_1 = 0.0643$
Final wR_2 indices (all data) ^[a]	$wR_2 = 0.1547$
Gof on F^2	1.018
Abs. structure parameter ^[b]	0.05(8)
Largest diff. peak and hole [e Å ⁻³]	0.565 and –0.481

[a] $R_1 = \sum |F_o| - |F_c| / \sum |F_o|$ and $wR_2 = \{\sum [w(F_o^2 - F_c^2)^2] / \sum [w(F_o^2)^2]\}^{1/2}$. [b] H. D. Flack, *Acta Crystallogr. Sect. A* **1983**, *39*, 876.

Preliminary unit cell constants were calculated with a set of 45 narrow-frame (0.3° in ω) scans. A total of 1271 frames of data were collected using the phi-omega scan method. The first 50 frames were recollected at the end of data collection to monitor for decay. The crystal used for the diffraction study showed no decomposition during data collection. Absorption corrections were applied by using the SADABS program^[27] (maximum and minimum transmission coefficients 0.9130 and 0.6608). The structure was solved by direct methods using the SHELXS-97 computer program^[28] for crystal structure determination and refined by full-matrix least-squares method on F^2 , with the SHELXL-97 computer program.^[29] 6599 reflections were included in the refinement and no restraints were applied to the 310 parameters. Hydrogen atoms were included in calculated positions and refined in riding mode. The weighting scheme employed was $w = [\sigma^2(F_o^2 + (0.0997P)^2 + 0.4457P)]$ and $P = (|F_o|^2 + 2|F_c|^2)/3$.

CCDC-274550 contains the supplementary crystallographic data for this paper. These data can be obtained free of charge from The Cambridge Crystallographic Data Centre via www.ccdc.cam.ac.uk/data_request/cif.

Computational Details: Calculations were carried out using the GAUSSIAN98 package.^[30] The hybrid density function method known as B3LYP was applied.^[31] Relativistic effective core potentials (ECP) from the Stuttgart–Dresden group were used to represent the innermost electrons of the ruthenium atoms.^[32] The basis set for the main group elements was split-valence and included a polarization function in all atoms (abbreviated as SVP).^[33] The geometries for the minima **13** and **14** were fully optimized in all the isomers. The search for transition states failed, and in an attempt to evaluate their relative stability we decided to make a partial optimization, which was performed by keeping the distances of the Ru...H...C fragment fixed at 1.75 and 1.38 Å, respectively.^[7] Some changes in these parameters were introduced without major changes in the relative stability of each family of compounds.

Acknowledgments

The authors thank Prof. Santiago Álvarez for constructive discussions. The authors also wish to thank the Ministerio de Educación y Ciencia (CTQ2004-01546/BQU and 2002-04033/BQU) and the Generalitat de Catalunya for financial support. The installation of the SMART CCD Single-Crystal Diffractometer at the University of A Coruña was supported by the Xunta de Galicia (XUGA INFRA-97).

- [1] For reviews see: a) D. Carmona, M. P. Lamata, L. A. Oro, *Eur. J. Inorg. Chem.* **2002**, 2239; b) M. J. Palmer, M. Wills, *Tetrahedron: Asymmetry* **1999**, *10*, 2045; c) G. Zassinovich, G. Messtroni, *Chem. Rev.* **1992**, *92*, 1051.
- [2] C. F. de Graauw, J. A. Peters, H. van Bekkum, J. Huskens, *Synthesis* **1994**, 1007.
- [3] a) M. Bernard, V. Guiral, F. Delbecq, F. Fache, P. Sautet, M. Lemaire, *J. Am. Chem. Soc.* **1998**, *120*, 1441; b) J.-E. Backwall, R. L. Chowdhuri, U. Karlsson, G. Z. Wang, in *Perspectives in Coordination Chemistry* (Eds.: A. F. Williams, C. Floriani, G. Merbach), Verlag Helvetica Chimica Acta, Basel, Switzerland, **1992**, p. 463.
- [4] a) R. Noyori, S. Hashiguchi, *Acc. Chem. Res.* **1997**, *30*, 97; b) K.-J. Haack, S. Hashiguchi, A. Fujii, T. Ikariya, R. Noyori, *Angew. Chem. Int. Ed. Engl.* **1997**, *36*, 285.
- [5] a) J.-X. Gao, T. Ikariya, R. Noyori, *Organometallics* **1996**, *15*, 1087; b) S. Hashiguchi, A. Fujii, S.-I. Inoue, T. Ikariya, R. Noyori, *J. Chem. Soc., Chem. Commun.* **1996**, 233.
- [6] a) P. Gamez, F. Fache, M. Lemaire, *Tetrahedron: Asymmetry* **1995**, *6*, 705; b) Y.-T. Jiang, Q.-Z. Jiang, X.-M. Zhang, *J. Am. Chem. Soc.* **1998**, *120*, 3817; c) M. Palmer, T. Walsgrove, M. Wills, *J. Org. Chem.* **1997**, *62*, 5226; d) Y.-B. Zhou, F.-Y. Tang, H.-D. Xu, X.-Y. Wu, J.-A. Ma, Q.-L. Zhou, *Tetrahedron: Asymmetry* **2002**, *13*, 469.
- [7] a) M. Yamakawa, H. Ito, R. Noyori, *J. Am. Chem. Soc.* **2000**, *122*, 1466; b) D. A. Alonso, P. Brandt, S. J. M. Nordin, P. G. Andersson, *J. Am. Chem. Soc.* **1999**, *121*, 9580.
- [8] M. Gómez, S. Jansat, G. Muller, M. C. Bonnet, J. A. J. Breuzard, M. Lemaire, *J. Organomet. Chem.* **2002**, *659*, 197.
- [9] Selected recent contributions: a) D. Franco, M. Gómez, F. Jiménez, G. Muller, M. Rocamora, M. A. Maestro, J. Mahía, *Organometallics* **2004**, *23*, 3197; b) J. A. Brito, M. Gómez, G. Muller, H. Teruel, J.-C. Clinet, E. Duñach, M. A. Maestro, *Eur. J. Inorg. Chem.* **2004**, 4278; c) M. Gómez, S. Jansat, G. Muller, M. A. Maestro, J. Mahía, *Organometallics* **2002**, *21*, 1077; d) M. A. Pericàs, C. Puigjaner, A. Riera, A. Vidal-Ferran, M. Gómez, F. Jiménez, G. Muller, M. Rocamora, *Chem. Eur. J.* **2002**, *8*, 4164.
- [10] a) M. K. Button, R. A. Gossage, *J. Heterocyclic Chem.* **2003**, *40*, 513; b) J. Castro, S. Cabaleiro, P. Pérez-Lourido, J. Romero, J. García-Vázquez, A. Sousa, *Polyhedron* **2001**, *20*, 2329; c) N. End, L. Macko, M. Zehnder, A. Pfaltz, *Chem. Eur. J.* **1998**, *4*, 818.
- [11] J. M. Canal, M. Gómez, F. Jiménez, M. Rocamora, G. Muller, E. Duñach, D. Franco, A. Jiménez, F. H. Cano, *Organometallics* **2000**, *19*, 966.
- [12] S. Cabaleiro, P. Pérez-Lourido, J. Castro, J. Romero, J. García-Vázquez, A. Sousa, *Transition Met. Chem.* **2001**, *26*, 709.
- [13] A. J. Davenport, D. L. Davies, J. Fawcett, S. A. Garratt, D. R. Russell, *J. Chem. Soc., Dalton Trans.* **2000**, 4432.
- [14] a) K. Stanley, M. C. Baird, *J. Am. Chem. Soc.* **1975**, *97*, 6598; b) R. S. Cahn, C. K. Ingold, V. Prelog, *Angew. Chem. Int. Ed. Engl.* **1966**, *5*, 385.
- [15] H. Brunner, B. Nuber, M. Prommesberger, *Tetrahedron: Asymmetry* **1998**, *9*, 3223.
- [16] A. Bondi, *J. Phys. Chem.* **1964**, *68*, 441.
- [17] M. D. Fryzuk, C. D. Montgomery, *Organometallics* **1991**, *10*, 467.

- [18] G. Aullón, D. Bellamy, L. Brammer, E. A. Bruton, A. G. Orpen, *Chem. Commun.* **1998**, 653.
- [19] W. J. Geary, *Coord. Chem. Rev.* **1971**, 7, 81.
- [20] M. Henning, K. Püntener, M. Scalone, *Tetrahedron: Asymmetry* **2000**, 11, 1849.
- [21] MACSPARTAN PRO Version 1.0.4. WaveFunction, Inc., 18401 Von Karman Avenue, suite 370, Irvine, CA 92612, U.S.A.
- [22] Blank tests using HCOOH/NEt₃ as hydrogen donor system showed that the amino-oxazoline ligands are not stable under these conditions.
- [23] D. G. I. Petra, P. C. J. Kamer, P. W. N. M. van Leeuwen, K. Goubitz, A. M. van Loon, J. G. de Vries, H. E. Schoemaker, *Eur. J. Inorg. Chem.* **1999**, 2335.
- [24] S. Hashiguchi, A. Fujii, K.-J. Haack, K. Matsumura, T. Ikaraya, R. Noyori, *Angew. Chem. Int. Ed. Engl.* **1997**, 36, 288.
- [25] R. Noyori, M. Tamakawa, S. Hashiguchi, *J. Org. Chem.* **2001**, 66, 7931.
- [26] W. L. F. Armarego, D. D. Perrin, *Purification of Laboratory Chemicals*, 4th ed., Butterworth-Heinemann, Oxford, UK, **1996**.
- [27] G. M. Sheldrick, SADABS, a program for empirical absorption correction of area detector data, University of Göttingen, Germany, **1996**. Based on the method of Robert Blessing: R. H. Blessing, *Acta Crystallogr., Sect. A* **1995**, 51, 33.
- [28] G. M. Sheldrick, SHELXS 97, a computer program for crystal structure determination, University of Göttingen, **1997**.
- [29] G. M. Sheldrick, SHELXL 97, a computer program for crystal structure refinement, University of Göttingen, **1997**.
- [30] M. J. Frisch, G. W. Trucks, H. B. Schlegel, G. E. Scuseria, M. A. Robb, J. R. Cheeseman, V. G. Zakrzewski, J. A. Montgomery Jr., R. E. Stratmann, J. C. Burant, S. Dapprich, J. M. Millam, A. D. Daniels, K. N. Kudin, M. C. Strain, O. Farkas, J. Tomasi, V. Barone, M. Cossi, R. Cammi, B. Mennucci, C. Pomelli, C. Adamo, S. Clifford, J. Ochterski, G. A. Petersson, P. Y. Ayala, Q. Cui, K. Morokuma, P. Salvador, J. J. Dannenberg, D. K. Malick, A. D. Rabuck, K. Raghavachari, J. B. Foresman, J. Cioslowski, J. V. Ortiz, A. G. Baboul, B. B. Stefanov, G. Liu, A. Liashenko, P. Piskorz, I. Komaromi, R. Gomperts, R. L. Martin, D. J. Fox, T. Keith, M. A. Al-Laham, C. Y. Peng, A. Nanayakkara, M. Challacombe, P. M. W. Gill, B. Johnson, W. Chen, M. W. Wong, J. L. Andres, C. Gonzalez, M. Head-Gordon, E. S. Replogle, J. A. Pople, Gaussian98 (Revision A.11), Gaussian Inc., Pittsburgh, PA, **2001**.
- [31] a) A. D. Becke, *J. Chem. Phys.* **1993**, 98, 5648; b) C. Lee, W. Yang, R. G. Parr, *Phys. Rev. B* **1988**, 37, 785.
- [32] D. Andrae, U. Haeussermann, M. Dolg, H. Stoll, H. Preuss, *Theor. Chim. Acta* **1990**, 77, 123.
- [33] A. Schafer, H. Horn, R. Ahlrichs, *J. Chem. Phys.* **1992**, 97, 2571.

Received: June 8, 2005

Published Online: September 21, 2005